similar papers at core.ac.uk

provided by Op

Open Archive Toulouse Archive Ouverte (OATAO)
OATAO is an open access repository that collects the work of Toulouse researchers and makes it freely available over the web where possible.

This is an author -deposited version published in: http://oatao.univ-toulouse.fr/
Eprints ID: 3835

To link to this article:

URL : **http://dx.doi.org/10.1016/j.tsf.2009.04.070**

To cite this version: Sarantopoulos, Christos and Gleizes, Alain and Maury, Francis (2009) *Chemical vapor deposition and characterization of nitrogen doped TiO2 thin films on glass substrates.* Thin Solid Films, vol. 518 (n° 4). 1299-1303 . ISSN 0040-6090

Any correspondence concerning this service should be sent to the repository administrator: staff-oatao@inp-toulouse.fr

Chemical vapor deposition and characterization of nitrogen doped TiO_2 thin films on glass substrates

Christos Sarantopoulos *, Alain N. Gleizes [1], Francis Maury [1]

CIRIMAT, CNRS–INPT–UPS, ENSIACET, 118 route de Narbonne, 31077 Toulouse cedex 4, France

A B S T R A C T

Photocatalytically active, N-doped TiO_2 thin films were prepared by low pressure metalorganic chemical vapor deposition (MOCVD) using titanium tetra-iso-propoxide (TTIP) as a precursor and NH_3 as a reactive doping gas. We present the influence of the growth parameters (temperature, reactive gas phase composition) on the microstructural and physico-chemical characteristics of the films, as deduced from X-ray diffraction (XRD), scanning electron microscopy (SEM), X-ray photoelectron spectroscopy (XPS), secondary ion mass spectrometry (SIMS) and ultra-violet and visible (UV/Vis) spectroscopy analysis. The N-doping level was controlled by the partial pressure ratio $R = [NH_3]/[TTIP]$ at the entrance of the reactor and by the substrate temperature. For $R = 2200$, the N-doped TiO_2 layers are transparent and exhibit significant visible light photocatalytic activity (PA) in a narrow growth temperature range (375–400 °C). The optimum N-doping level is approximately 0.8 at.%. However, the PA activity of these N-doped films, under UV light radiation, is lower than that of undoped TiO_2 films of comparable thickness.

Keywords:
MOCVD
Titanium dioxide
Nitrogen doping
Visible light photocatalysis
Glass coating

1. Introduction

Titanium dioxide (TiO_2) is extensively used in modern life applications, e.g. cosmetics, pigments, building materials, antibacterial surfaces, biocompatible material for prosthesis and solar cells [1–4]. Many research works of the past two decades focus on the photocatalytic properties of this semi-conducting transparent material. Under UV light (wavelength < 387 nm) TiO_2-anatase leads to the degradation and total mineralization of a great number of pollutants dispersed in air or water [5]. Moreover, the photo-induced super-hydrophilicity of TiO_2 films has also been achieved under UV light [6]. These two properties are very attractive: a thin film of TiO_2 can decompose atmospheric pollutants present on its surface and get self-cleaning from any dust and organic residues at the same time. Thus, the coating of large glass surfaces with TiO_2 (buildings, cars, etc.) is a smart way to decrease maintenance costs and contribute to the cleaning of urban air. Considering that the UV light is only 5% of the sun spectrum, real commercial applications will drastically develop if activation of these semi-conducting films by the visible light is enhanced.

A simple idea to activate the TiO_2 photocatalyst by the visible light is to reduce the band gap (initially 3.2 eV for TiO_2-anatase) by inserting intermediate electronic states in the band gap of the electronic structure. This can be achieved by creating defects, i.e. oxygen vacancies (TiO_{2-x}) or atoms in substitution or insertion (cationic and anionic doping). Oxygen deficient TiO_{2-x} films produced by MOCVD [7] and powders produced by TiC, TiN, TiO and Ti_2O_3 oxidation [8], gave positive results. Doping of TiO_2 anatase powders with Fe [9], Cr [10] and Ag [11] led to visible photocatalytic decomposition of oxalic acid, yellow XRG dye and rhodamine B, respectively. The optimum doping level reported so far is quite low (e.g. $Fe^{+3} = 0.09\%$ or Fe/Ti = 0.05 [9]). TiO_{2-x} and cation-doped TiO_2 samples suffer from thermal stability and low photocatalytic activity because of the presence of uncontrolled structural defects which act as electron and hole traps [12].

Concerning anion doping, recently Asahi et al. [13] proposed an interesting approach for elaborating N-doped TiO_2 anatase films by substituting oxygen with nitrogen atoms. The small difference between nitrogen and oxygen ion radii facilitates nitrogen substitution and does not distort the crystal lattice much. Theoretical modeling was also used to demonstrate that the semiconductor band gap decreases when the N 2p states mix with the O 2p states, thus rendering the material active under visible light [13,14]. Still, the electronic structure of the efficient nitrogen doped anatase is under question [8,15,16]. Despite the great number of scientific reports about N-doped TiO_2 thin films, only few works mention successful results for supported thin layers. F.-D. Duminica et al. have proposed an atmospheric pressure CVD process (APCVD) for the growth of pure TiO_2 [17] and further, by using N_2H_4 as doping reactive gas, they have reported significant photocatalytic activity in the visible light range but for films deposited in narrow growth conditions [18]. Working with APCVD but using NH_3 as a reactive gas instead, Yates et al. found no evidence of photocatalytic activity [19]. However Maeda et al. [20]

* Corresponding author. Current address: IRCELYON–CNRS, 2 Avenue Albert Einstein, 69626 Villeurbanne cedex, France. Tel.: +33 4 72 44 53 62; fax: +33 4 72 44 53 99.
E-mail addresses: christos.sarantopoulos@gmail.com (C. Sarantopoulos), Alain.Gleizes@ensiacet.fr (A.N. Gleizes), Francis.Maury@ensiacet.fr (F. Maury).
[1] CIRIMAT, ENSIACET, 118 route de Narbonne, 31077 Toulouse cedex 4, France.

Table 1
Typical MOCVD conditions used for the growth of N-doped TiO_2 layers.

Growth temperature (°C)	300–425
Pressure (Torr)	20
Carrier gas flow rate (N_2, sccm)	20
NH_3 gas flow rate (sccm)	25–100
NH_3/TTIP	555–2220
Total gas flow rate (sccm)	600
Bubbler temperature TTIP (°C)	25
TTIP molar fraction (10^{-6})	65
Deposition time (min)	180–360
Substrate	Borosilicate glass, Si(100)

reported visible light activity of films prepared by plasma enhanced CVD under low pressure and using NH_3 as reactive gas. Efficient photocatalysts under visible light were also produced using other deposition methods such as ion-assisted electron-beam evaporation [21] or magnetron sputtering [13,22].

This work reports the growth of photocatalytically active N-doped TiO_2 films by low pressure CVD on glass substrates, using titanium tetra-iso-propoxide (TTIP) as titanium and oxygen precursor and NH_3 as nitrogen source. The microstructural characteristics and the photocatalytic activity of the films are discussed in relation with the growth parameters.

2. Experimental

A horizontal hot-wall CVD quartz reactor 5 cm in diameter was used for the film deposition. Borosilicate flat glass and Si(100) wafers were placed on an inclined stainless steel sample holder at a distance 14 cm from the entrance. The main precursor decomposition zone, found from preliminary runs, is extended from 11 to 18 cm from the entrance of the reactor. The growth temperature was controlled by a thermocouple K plugged into the sample holder. Liquid TTIP was placed in a bubbler thermostated in a water bath at 298 K. Pure N_2 (99.9992%) was fed through two lines equipped with mass flow controllers, one to bubble through the TTIP precursor, the other to dilute it. The total pressure was maintained at 20 Torr. For the N-doping, NH_3 gas (99.999%) was fed through the reactor during the deposition. Table 1 presents the typical MOCVD conditions. The film microstructure was studied by X-ray diffraction (XRD) using θ-θ and grazing geometry (Cu Kα). The surface morphology was observed by scanning electron microscopy (SEM) and the film thickness was determined on cross sections and by optical methods [23]. The arithmetical average of the surface roughness profile (R_a) was measured using an optical interferometer. The film composition was analyzed by secondary ion mass spectrometry (SIMS) and X-ray photoelectron spectroscopy (XPS). Optical properties were determined using a UV–Vis spectrophotometer equipped with an integrating sphere. The band gap (E_g) was determined by extrapolation of the absorption edge using Tauc's plot.

The photocatalytic activity of the one-side coated borosilicate flat glass (32×32 mm^2) was determined from the initial decomposition rate (r_0) of an aqueous Orange G solution (10^{-5} mol L^{-1}) under UV and visible irradiation. The sample immersed in 25.0 cm^3 of the dye solution was placed into a quartz vessel (28.8 cm^3) transparent to wavelengths >290 nm. All solutions were first agitated for 1 h in the dark in order to reach equilibrium with the photocatalyst. The concentration was determined by measuring the absorbance of Orange G at 480 nm and applying the Beer–Lambert law. The kinetic curves of Orange G decomposition were obtained by plotting the concentration as a function of irradiation time. The r_0 was determined by the slope of the linear fitting over the first 60 min for UV irradiation and over the first 360 min for the visible light irradiation. For UV tests the sample was irradiated with 1.05 mW cm^{-2} (365 nm) using a UV lamp (HPLN Philips 125 W). The tests under visible light were performed using two fluorescent lamps (FCE27 52 W) coupled with a UV cut filter (400 nm) providing a cumulative irradiance in the range 450–550 nm of 14.1 mW cm^{-2}. The results of the structural analysis (XRD), photocatalytic activity and optical properties refer to films deposited on borosilicate glass substrates while composition analysis (SIMS, XPS) and SEM observations were performed on films grown on Si (100) wafers.

3. Results and discussion

3.1. Growth rate

Fig. 1 shows the variation of the growth rate of undoped and N-doped TiO_2 films with the substrate temperature using a partial pressure ratio NH_3/TTIP of $R=2220$. Below 350 °C the growth rate is enhanced when NH_3 is added. Above 350 °C the growth rate increases slowly with the temperature both in presence of and without NH_3. Above this temperature threshold, the growth rate of undoped and N-doped films cannot be compared directly because the TTIP mole fraction is different. However, we observed that above 350 °C the growth rate of undoped-TiO_2 is approximately 4 times higher than that of N-doped TiO_2 (2 and 8 nm min^{-1}, respectively) which is certainly due to the fact that the TTIP mole fraction was 4 times higher for the growth of undoped layers. As a result, we assume the growth rate would be probably of the same order at high temperature if the same TTIP mole fraction had been used. By contrast, for deposition temperatures lower than 350 °C, the growth rate of N-doped TiO_2 is of the same order (or even higher at 300 °C) despite the higher TTIP mole fraction used for undoped TiO_2 films. In fact, the apparent activation energy for the deposition of N-doped TiO_2 films is very low (13 kJ mol^{-1}) comparatively to that of pure TiO_2 films (93 kJ mol^{-1}). This suggests that in the presence of NH_3 the process is not kinetically controlled as a result of fast reactions between NH_3 and TTIP. This is consistent with the observations of Jung et al. who considered that the decomposition of TTIP was catalyzed by NH_3 (direct interaction of NH_3 with electron deficient Ti in TTIP) leading to higher decomposition rates at temperatures lower than 330 °C [24].

3.2. Morphology, structure and composition

From X-ray diffraction patterns, the N–TiO_2 films grown above 350 °C using $R=2220$ are well crystallized while those prepared at temperatures equal to or lower than 350 °C contain a significant part of amorphous phase. All films exhibit the anatase structure and are constituted of nano-crystals of various sizes. For growth temperatures

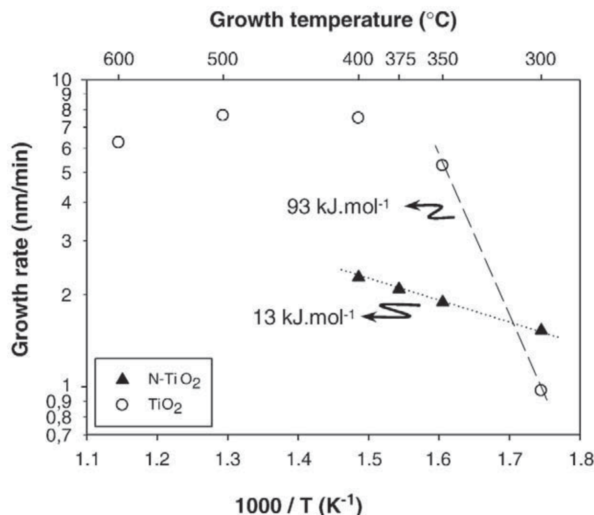

Fig. 1. Arrhenius plot of the growth rate of N-doped and pure TiO_2 films grown on Si(100) wafers using TTIP mole fractions of 65×10^{-6} (N–TiO_2) and 260×10^{-6} (TiO_2).

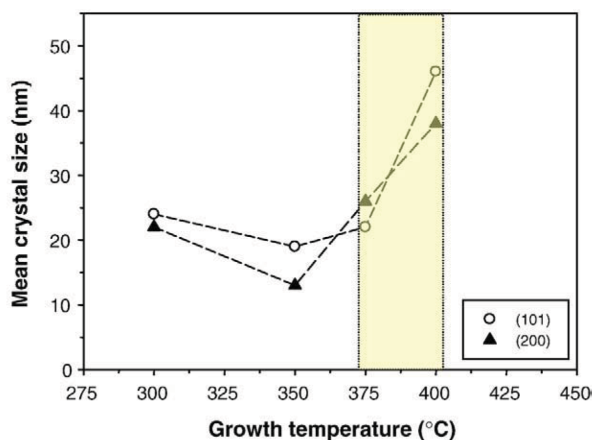

Fig. 2. Influence of the growth temperature on the mean crystal size of N-doped TiO_2 films determined from the FWHM of the (101) and (200) anatase XRD peaks ($R = 2200$).

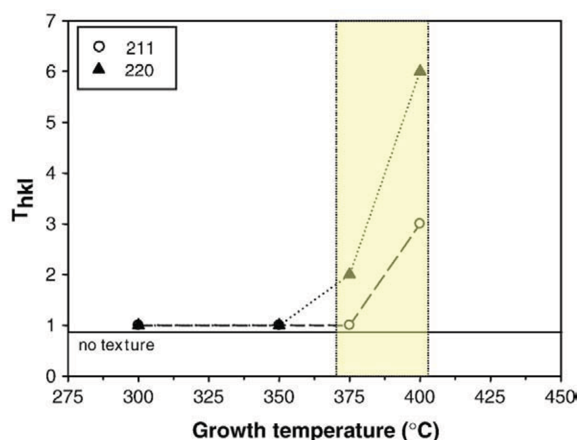

Fig. 4. Variation of texture coefficient in the (211) and (220) direction with the growth temperature for N-doped TiO_2 films grown with $R = 2200$.

between 300 °C and 350 °C, the mean crystal size is small (20 ± 5 nm) and does not change much with the temperature (Fig. 2). Increasing the growth temperature up to 400 °C leads to significant increase of the crystal size (40 ± 5 nm).

Surface morphology reveals that the small TiO_2 crystals are agglomerated to form grains. The grain size, as determined by surface SEM observations, increases with the film thickness, i.e. with the deposition time because of crystal growth and aggregation phenomena during the growth (Fig. 3). The oxide layers prepared at low temperature (300 and 350 °C) are made of large aggregates of small crystals (namely grains) and present a compact granular morphology. The films prepared above 350 °C exhibit a uniform columnar morphology. This change in film morphology leads to a decrease of the surface grain size when the temperature increases from 300 to 400 °C. Taylor et al. reported a similar grain size variation versus deposition temperature [25]. These last samples show texture in the (211) and (220) directions whereas no preferential orientation is found for the granular morphology grown at and below 350 °C (Fig. 4). This is correlated with the change of film morphology above 350 °C, followed by the improvement of crystallinity. The surface roughness of N-doped TiO_2 films decreases when the growth temperature increases: $R_a =$ 177 nm, 107 nm and 21 nm for films prepared at 300 °C, 350 °C and 400 °C, respectively.

The N-doping level of the films is controlled by varying the mole fraction ratio R as well as the growth temperature. Even for low values of R (555), SIMS analysis shows that nitrogen is incorporated into the film (Fig. 5). The N concentration profile is constant through the film thickness, suggesting homogeneous doping. Fig. 6 shows that for high R values (2200), the relative N content is maximized for a growth temperature of 350 °C and decreases near to the detection limit when the temperature is 400 °C. The relative N content was estimated by XPS at 4.8 and 0.8 at.% for the growth temperature of 350 and 400 °C, respectively. At low temperatures (equal or inferior to 350 °C) the catalytic reaction of TTIP with NH_3, leads to the incorporation of high amounts of N species [24]. At higher growth temperatures ($T > 375$ °C) the pyrolytic self-decomposition of TTIP becomes dominant and faster than NH_3 decomposition leading to growth of TiO_2 films with a relatively low N incorporation. Additionally, competitive reactions as N is released from growing films may occur as observed during thermal treatment in air at 450 °C of TiO_xN_y [26].

In XPS spectra, the N 1s level is found at 396 eV for films grown below 400 °C. According to [13], it is attributed to N atoms substituting for O atoms. For N–TiO_2 films deposited at 400 °C and above, this N 1s peak at 396 eV is not observed maybe because of the very low N incorporation (0.8 at.%). In these conditions, a small N 1s peak is detected at 400 eV which corresponds to chemisorbed nitrogen [13,27,28].

3.3. Optical properties

Changes in composition are also reflected in the optical properties of the films. The absorption of light by the films is shifted to the visible

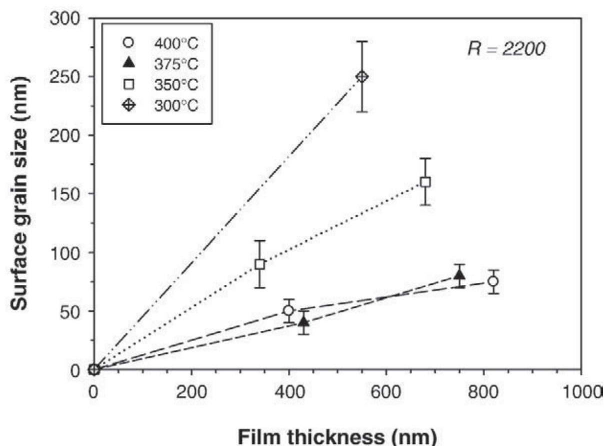

Fig. 3. Variation of the surface grain size of N-doped TiO_2 films with the thickness for various growth temperatures using $R = 2200$.

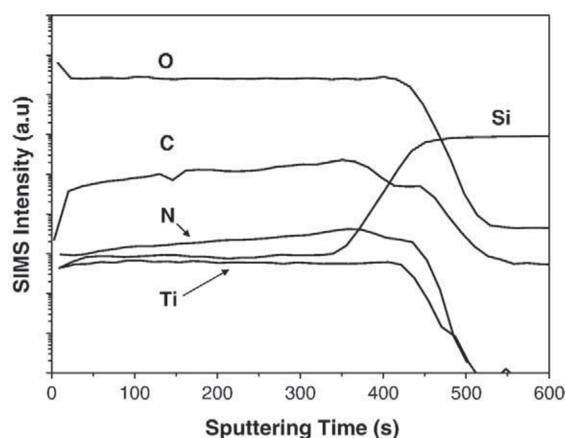

Fig. 5. SIMS profiles of an N-doped TiO_2 film grown on Si(100), at 300 °C, using $R = 555$ (film thickness = 200 nm).

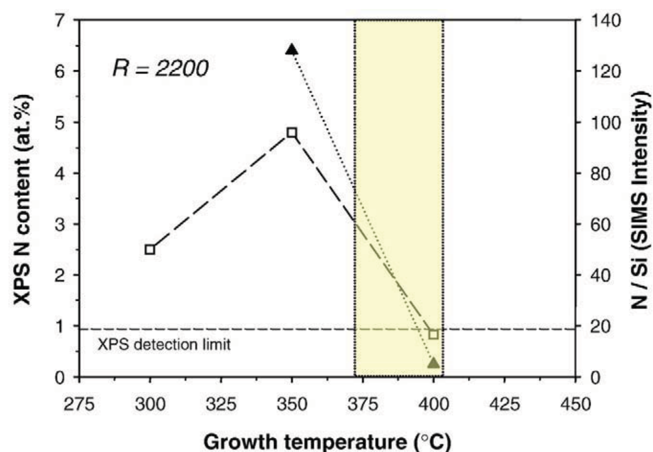

Fig. 6. Variation of the nitrogen content of N-doped TiO_2 films with the growth temperature for $R = 2200$. Left-axis: N atomic percentage as determined by XPS analysis (□). Right-axis: SIMS N/Si intensity ratio (▲) determined after Ar^+ sputtering to eliminate the surface contamination (film thickness ~200 nm).

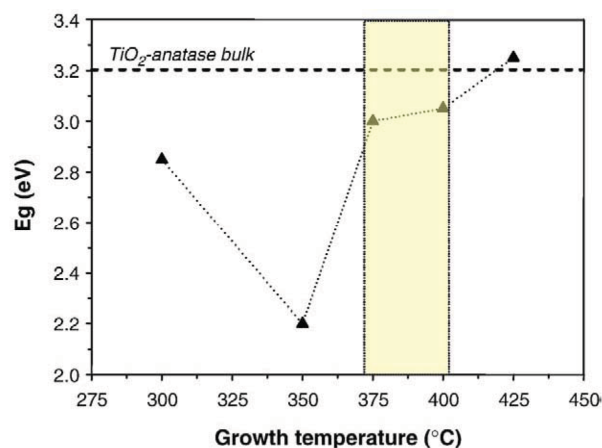

Fig. 8. Variation of the optical band gap with growth temperature for N-doped TiO_2 films grown with $R = 2200$ (the dotted line is for bulk anatase band gap).

range when the quantity of ammonia is increased in the gas phase (Fig. 7). Simultaneously, the aspect of the films changes from transparent and colorless ($R = 0$) to green colored ($R = 2200$). The shift to the visible light region is also observed for all films of comparable thickness grown between 300 °C and 425 °C, even if not systematically marked by the above mentioned color change. With $R = 2200$, the color depends on growth temperature. The films prepared at 300 °C are light yellow and not very transparent (23%). Those prepared at 350 °C are light green and not transparent (6%). Those prepared between 375 °C and 425 °C are colorless and transparent (50–85%). Raising the quantity of ammonia ($R = 4000$) in the gas phase, leads to dark brown films with a metallic lustre. For all N-doped TiO_2 films the fundamental absorption edge was shifted to the visible range. Fig. 8 shows that the optical band gap variation with the growth temperature is not continuous. For a growth temperature of 300 °C, the band gap is 2.85 eV and it decreases to 2.20 eV when the growth temperature is 350 °C. Samples prepared at 375 °C and above show larger optical band gaps increasing from 3.00 eV to 3.25 eV. The latter value corresponds to pure anatase. The semiconductor band gap varies also with the grain size of the film [29,30]. However for the grain size values of the films studied here (50–250 nm), no significant influence is considered. These results are more likely consistent with the variation of the N content with the growth temperature (Fig. 6): the more nitrogen the structure incorporates, the narrower the band gap gets.

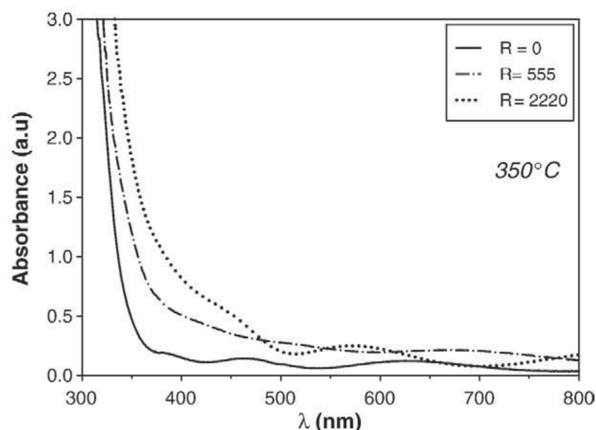

Fig. 7. Optical absorption spectra of N-doped TiO_2 films prepared at 350 °C using various R ratios (film thickness = 300–350 nm).

3.4. Photocatalytic activity

Figs. 9 and 10 show the photocatalytic activity of N-doped TiO_2 samples under UV and visible light irradiation. All films were deposited on glass substrates of same dimensions (32×32 mm^2) at temperatures between 300 °C and 450 °C, using $R = 2200$. They have

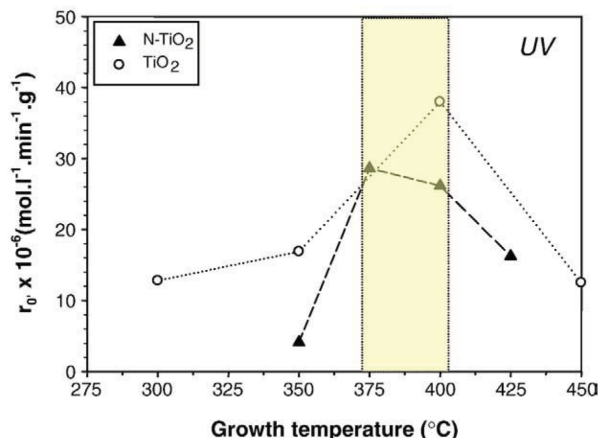

Fig. 9. Variation of the normalized initial photocatalytic decomposition rate under UV light radiation with growth temperature for N-doped ($R = 2200$) and pure TiO_2 films.

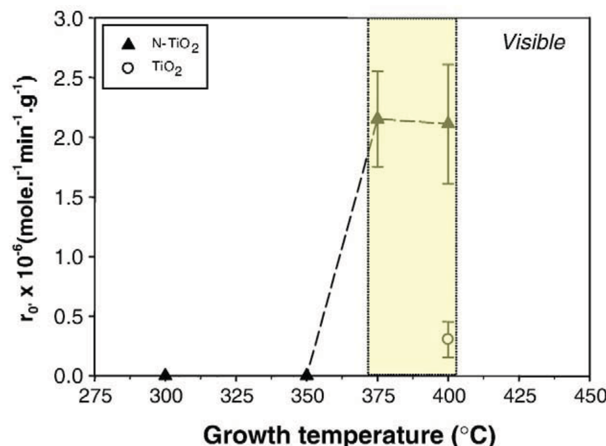

Fig. 10. Variation of the normalized initial photocatalytic decomposition rate under visible light radiation with growth temperature for N-doped ($R = 2200$) and pure TiO_2 films.

approximately the same thickness. In order to compare the photocatalytic activity of the samples, the initial decomposition rate r_0 was normalized by the mass of deposited photocatalyst (r_0' in mol L^{-1} min^{-1} g^{-1}). Non doped TiO_2 films of same thickness were also tested and compared with the N-doped ones. It is generally observed that raising the growth temperature leads to films with higher photocatalytic activity. Under UV irradiation the activity of all N-doped TiO_2 films is lower than that of pure TiO_2 films (Fig. 9). The most efficient samples under UV irradiation (N-doped and pure TiO_2 films) were obtained at 375–400 °C. The decrease of r_0' for the films elaborated at 425 °C and above is due to the poor crystallization of the film originating from the glass surface thermal softening.

Under visible light radiation, the overall decomposition rates of Orange G on N-doped TiO_2 films are lower than under UV irradiation. Comparing with the non doped films grown at 400 °C, it appears that N-doping enhances photocatalytic activity in the visible light by a factor of 10. The best visible activity is obtained for films prepared in the narrow window 375–400 °C. This temperature range is slightly lower than in our previous work using N_2H_4 as nitrogen source [18]. This result is to be correlated with the composition modification of TiO_2 films containing a small quantity of nitrogen (0.8 at.%) leading to a slight band gap shrinkage (3.00–3.05 eV) with respect to that of pure anatase (3.25 eV). The films prepared at 300 °C and 350 °C are photocatalytically inactive both under UV and visible light. This is explained by the low crystallinity of the films and the high content in incorporated nitrogen which act as defects favoring carrier recombination rather than efficient doping.

4. Summary and conclusions

N-doped TiO_2 films, photocatalytically active under visible and UV light were grown by low pressure CVD process using TTIP as a precursor and NH_3 as a reactive gas. A narrow window of the growth parameters was found for a PA in the visible range. This results from a compromise between the crystallinity and the nitrogen content of these transparent TiO_2 films grown on glass substrate. The optimal N content was found below 1 at.% for well crystallized anatase prepared at 375–400 °C. Other works have reported effective doping level of substitutional nitrogen between 1 and 2% [21,22]. Higher N concentrations result in a high level of structural defects that behave as charge (electron, holes) recombination centers.

References

[1] A. Nasu, Y. Otsubo, J. Colloid Interface Sci. 310 (2007) 617.
[2] P. Evans, D.W. Sheel, Surf. Coat. Technol. 201 (2007) 9319.
[3] S. Popescu, I. Demetrescu, C. Sarantopoulos, A.N. Gleizes, D. Iordachescu, J. Mater. Sci.: Mater. Med. 19 (2008) 1451.
[4] L. Schmidt-Mende, M. Grätzel, Thin Solid Films 500 (2006) 296.
[5] A. Fujishima, K. Hashimoto, T. Watanabe, TiO2 Photocatalysis: Fundaments and Applications, BKC, Tokyo, May 1999.
[6] T. Watanabe, A. Nakajima, R. Wang, M. Minabe, S. Koizumi, A. Fujishima, K. Hashimoto, Thin Solid Films 351 (1999) 260.
[7] I. Justicia, P. Ordejón, G. Canto, J.L. Mozos, J. Fraxedas, G.A. Battiston, R. Gerbasi, A. Figueras, Adv. Mater. 14 (2002) 1399.
[8] I.N. Martyanov, S. Uma, S. Rodrigues, K.J. Klabunde, Chem. Commun. 21 (2004) 2476.
[9] W.Y. Teoh, R. Amal, L. Madler, S.E. Pratsinis, Catal. Today 120 (2007) 203.
[10] J. Zhu, Z. Deng, F. Chen, J. Zhang, H. Chen, M. Anpo, J. Huang, L. Zhang, Appl. Catal., B 62 (2006) 329.
[11] H.M. Sung-Suh, J.R. Choi, H.J. Hah, S.M. Koo, Y.C. Bae, J. Photochem. Photobiol., A 163 (2004) 37.
[12] W. Choi, A. Termin, M.R. Hoffmann, J. Phys. Chem. 98 (1994) 13669.
[13] R. Asahi, T. Morikawa, T. Ohwaki, K. Aoki, Y. Taga, Science 293 (2001) 269.
[14] M. Miyauchi, A. Ikezawa, H. Tobimatsu, H. Irie, K. Hashimoto, Phys. Chem. Chem. Phys. 6 (2004) 865.
[15] H. Irie, S. Washizuka, N. Yoshino, K. Hashimoto, Chem. Comm. 11 (2003) 1298.
[16] I. Nakamura, N. Negishi, S. Kutsuna, T. Ihara, S. Sugihara, K. Takeuchi, J. Mol. Catal. A: Chem. 161 (2000) 205.
[17] F.-D. Duminica, F. Maury, F. Senocq, Surf. Coat. Technol. 188–189 (2004) 255.
[18] F.-D. Duminica, F. Maury, R. Hausbrand, Surf. Coat. Technol. 201 (2007) 9349.
[19] H.M. Yates, M.G. Nolan, D.W. Sheel, M.E. Pemble, J. Photochem. Photobiol., A 179 (2006) 213.
[20] M. Maeda, T. Watanabe, J. Electrochem. Soc. 153 (2006) C186.
[21] M.-C. Yang, T.-S. Yang, M.-S. Wong, Thin Solid Films 469–470 (2004) 1.
[22] M.-S. Wong, H. Pang Chou, T.-S. Yang, Thin Solid Films 494 (2006) 244.
[23] C. Sarantopoulos, Ph.D. Thesis, INP Toulouse, 2007 (http://ethesis.inp-toulouse.fr/archive/00000545/01/sarantopoulos.pdf).
[24] S.-H. Jung, S.-W. Kang, Jpn. J. Appl. Phys. 40 (2001) 3147.
[25] C.J. Taylor, D.C. Gilmer, D.G. Colombo, G.D. Wilk, S.A. Campbell, J. Roberts, W.L. Gladfelter, J. Am. Chem. Soc. 121 (1999) 5220.
[26] F.D. Duminica, F. Maury, Surf. Coat. Technol. 202 (2008) 2423.
[27] C. Guimon, A. Gervasini, A. Auroux, J. Phys. Chem., B 105 (2001) 10316.
[28] N.C. Saha, H.G. Tompkins, J. App. Phys. 72 (1992) 3072.
[29] G.-L. Tian, H.-B. He, J.D. Shao, Chin. Phys. Lett. 22 (7) (2005) 1787.
[30] X.K. Zbao, J.H. Fendler, J. Phys. Chem. 95 (1991) 3716.